



## A train of kink folds in the surficial salt of Qom Kuh, Central Iran

John W. Cosgrove<sup>a,\*</sup>, Christopher J. Talbot<sup>b</sup>, Pedram Aftabi<sup>c</sup>

<sup>a</sup> Department of Earth Science and Engineering, Imperial College of Science, Technology & Medicine, Royal School of Mines, Prince Consort Road, London SW7 2AZ, UK

<sup>b</sup> Department of Earth Sciences, Uppsala University, SE-752 36 Uppsala, Sweden

<sup>c</sup> Geological Survey of Iran, PO Box 131851-1494, Tehran, Iran

### ARTICLE INFO

#### Article history:

Received 18 September 2008

Received in revised form

18 June 2009

Accepted 29 June 2009

Available online 8 July 2009

#### Keywords:

Salt extrusion

Iran

Dilated carapace

Mechanical anisotropy

Kink folds

Chevron folds

### ABSTRACT

The many subaerial extrusions of salt current in Iran are smaller and faster versions of steady state extrusions of metamorphic rocks from crustal channels in mountain chains. The extruded salt develops a variety of internal folds as the salt accumulates ductile displacements that can reach metres a year. Weather-induced elastic strains de-stress the outer layers of salt extrusions to a brittle carapace of broken dilated salt. Qom Kuh, situated in Central Iran, is a comparatively small and slow example of a viscous salt fountain and, as a result, its brittle elastic carapace may be thicker than most. This may account for Qom Kuh being the only salt fountain known to have a train of 10 m scale kink folds in its surficial salt. We attribute these folds to lateral shortening and back-shear of a surface-parallel planar mechanical anisotropy in the surficial salt induced by gravitationally driven ductile flow of the underlying salt. When it is dry, the elastic carapace is relatively strong and acts as a stiff corset impeding gravity spreading of the underlying confined salt. However, the carapace weakens and kinks on wetting, allowing the underlying salt to gravity spread. These folds illustrate how the weather can affect gravity spreading of surficial salt masses and how complex the interplay of tectonic and climatic signals can be in “steady state” mountains.

© 2009 Elsevier Ltd. All rights reserved.

### 1. Introduction

Like ice, salt is one of the weakest rocks. Thin salt layers lubricate regional décollements and thick salt layers feed diapirs, some of which extrude and gravity spread over the surface. Active subaerial salt extrusions are smaller and faster natural models of “steady state” mountains of other metamorphic rocks that extrude from infrastructural channels in the crust (e.g. Beaumont et al., 2001). Of particular relevance to the present study is the insight that extruded salt provides into the mechanisms and relative timing of the various types of folds found within extruded metamorphic rocks.

Qom Kuh is a mountain of Eocene–Oligocene salt in Central Iran, Fig. 1 (see e.g. Talbot and Aftabi, 2004). Like other active subaerial extrusions of salt in Iran (Talbot, 1998; Bahroudi and Talbot, 2003), Qom Kuh has the smooth outline of a viscous fountain (Lister and Kerr, 1989) with a summit dome feeding a topographically-lower apron of allochthonous salt gravity spreading over younger country rocks on length scales of kilometres and time scales of  $1-10^{5-6}$  years.

Gravity ( $\pm$ lateral tectonic stresses) drives salt from subsurface source-layers, up steep diapiric channels and out of vents partially collared by upturned country rocks (Hudec and Jackson, 2007). Most of the diapirs currently extruding in Iran are reactive and rise along dilational zones generated at releasing bends along N–S striking strike-slip faults that act as transfer faults in the Zagros Mountains (see e.g. Sepehr and Cosgrove, 2005) and W–E striking regional faults in the Central Iranian plateau (Talbot and Alavi, 1996). Salt extruded above any laterally surrounding collar cannot support its own weight in air and gravity spreads over the surrounding landscape as a crystalline viscous fluid (e.g. Fig. 1).

Salt extrusions in Iran tend to evolve through similar stages whether they consist of Hormoz (Neoproterozoic–Cambrian) salt in the eastern Zagros (Talbot, 1998) or Eocene–Oligocene salt in Central Iran. Thus domes of country rocks above blind diapirs are pierced by dykes of salt (Player, 1969) that rise to young, extruding topographic salt domes that mature to the smooth profiles of vigorous viscous fountains. After salt fountains have locally depleted their source layer, their summit domes subside and they assume the distinctive profiles of viscous droplets (Huppert, 1982) up to 10 km across. The rainfall then slowly degrades salt droplets into piles and eventually badlands of residual insoluble soils  $\pm$  blocks extruded with the salt. Salt fountains range in symmetry from axisymmetric (like a fried egg) where they spread over a plain,

\* Corresponding author. Tel.: +44 20 7594 6466; fax: +44 20 7594 7444.  
E-mail address: [j.cosgrove@imperial.ac.uk](mailto:j.cosgrove@imperial.ac.uk) (J. W. Cosgrove).

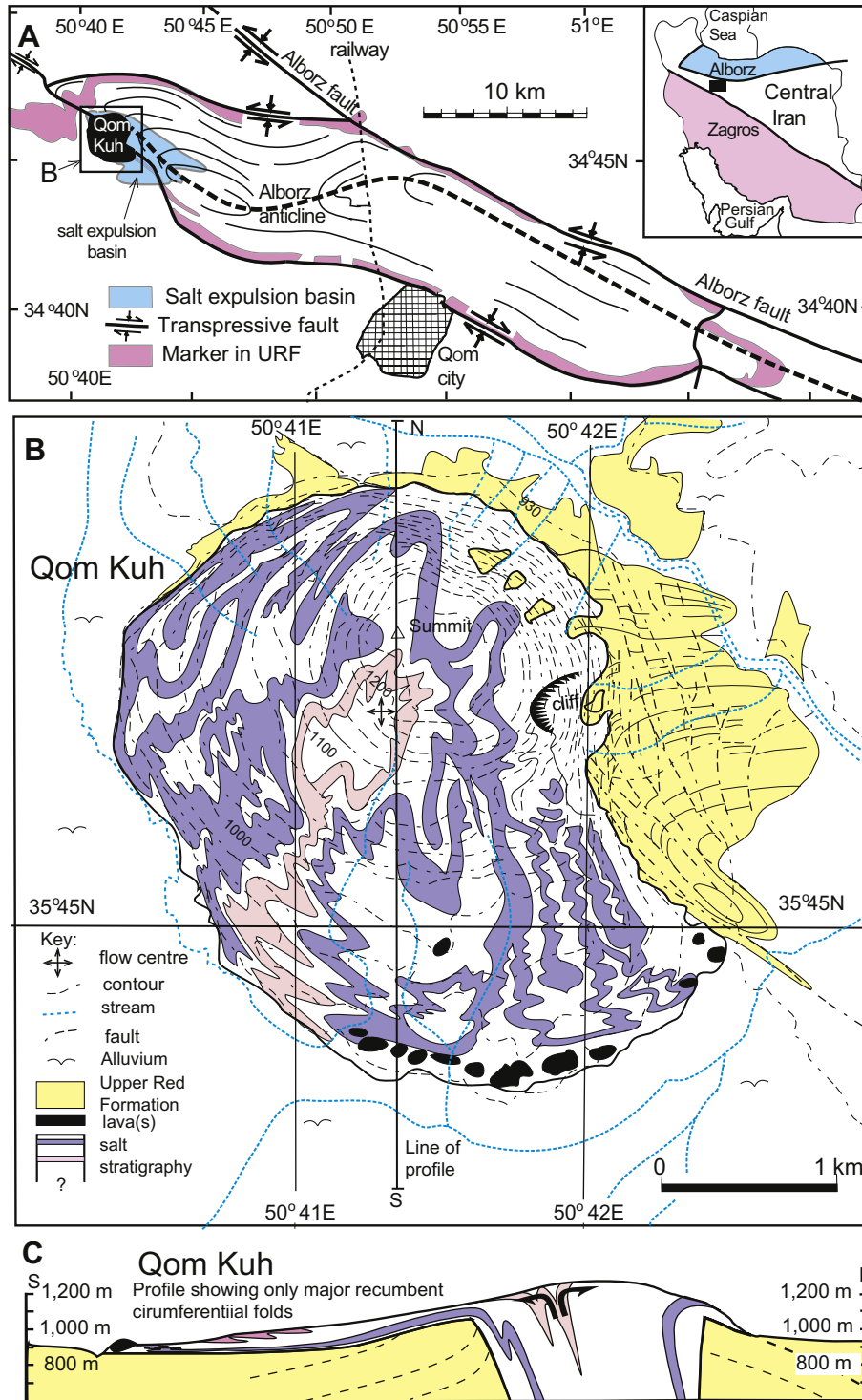


**Fig. 1.** Geology of Qom Kuh, central Iran. A. Map showing regional structural setting. Insert relates location to orogenic belts in Iran (from Talbot and Aftabi, 2004). B. Geological map. Stratigraphy shown in salt is arbitrary to show the general pattern of folds in the salt. Topographic contour intervals are 20 m. C. The S–N profile has no vertical exaggeration and is located on B. Black arrows indicate flow separation point off-centred from summit.

through orthorhombic, feeding two namakiers (salt glaciers) down both flanks of an anticline, to monoclinic, feeding one namakier flowing down one anticlinal flank. The advance of the distal margin of an axisymmetric viscous fountain slows as it spreads over a horizontal surface. By contrast, a monoclinic fountain spreading downslope can maintain a constant rate of advance until its distal salt is dissolved or buried.

Qom Kuh, the salt extrusion examined in this paper, is a slightly asymmetric fountain feeding allochthonous salt preferentially to the W and S from a stem plunging steeply to the NE (Fig. 1). Most of Qom Kuh consists of multicoloured salt that has been extruding for ~42,000 years from the base of the Oligocene to Miocene Upper Red Formation salt about 3 km deep (Talbot and Aftabi, 2004). The extruded multicoloured salt largely obscures earlier flows of an

older sequence of white salt that probably extruded from the base of the 6 km deep Eocene Lower Red Formation (Talbot and Aftabi, 2004).

Fountains of the much older Hormoz (Neoproterozoic–Cambrian) salt in the Zagros can extrude out of their vents at over  $1 \text{ m a}^{-1}$  and rise 400 m above the surrounding country rocks (e.g. Talbot et al., 2000). By comparison, Qom Kuh is slow and small for its salt currently rises only 315 m above the surrounding plain. Assuming steady state salt fountains to share dynamic similarity, Talbot and Aftabi (2004), estimated that Qom Kuh extrudes out of its vent at  $\sim 8 \text{ cm a}^{-1}$ ,  $\sim 4$  times faster than the average rainfall of  $23 \text{ mm a}^{-1}$  could theoretically dissolve it.

## 2. Bedding as a passive marker illustrating folding in salt

Mechanically passive colour layers in the salt (presumably deformed bedding) exhibit five types of folds in extruded salt. These are: sheath and curtain folds inherited from deformation in the source and diapir, tank-track folds, flow folds, and kink folds. The occurrence of four of these fold types in salt diapirs is comparatively well understood based on analogue models (e.g. Talbot and Aftabi, 2004). Two of them (curtain folds and tank-track folds) form because of changes in the boundary conditions operating on viscous flow. The formation of others (flow folds) reflects changes in the relative rates of salt drive and gravity spreading. After outlining the first four types of folds that occur in all Iranian salt extrusions, we focus on the kink folds that appear to be unique to Qom Kuh and treat them as a special category. These kink folds have been mentioned previously (Talbot and Aftabi, 2004) but have not been described, explained or modelled adequately.

Salt rising up the diapir at Qom Kuh splits into two unequal flow folds visible in profiles of the summit dome, a small one facing north and a larger one facing south and west (Fig. 1C). As it passes through the flow separation zone a few hundred metres southwest of the summit, the salt undergoes strong divergent lateral extension that thins the initial salt stratigraphy and imposes a strong surface-parallel foliation. In addition to this foliation, salt emerges on Qom Kuh with curtain folds already built into it. Experiments suggest that these folds initiate with radial subvertical axial surfaces and subhorizontal axes as a result of channel flow in the source layer converging on the base of the diapiric stem (Ramberg, 1981, pp. 311–312). The axes of such upright folds turn to subvertical with subvertical radial axial surfaces as they are carried up the diapiric stem as curtain folds. Instead of opening in the radial extensional flow in the extruded salt fountain, their axial surfaces rotate to parallel the top free surface of the salt and traces of them are recognisable even in the most distal allochthonous salt. Similarly, sheath folds generated anywhere in the flowing salt are presumably among the few recumbent folds with axes close to the flow direction.

Whatever its symmetry, the top free surface of a viscous fountain spreading sub aerially flows downslope, rolls over its advancing flow front and attaches to its substrate. As a result, colour layers in the flowing fluid develop a single basic *tank-track fold*. This has an axis that parallels the flow front and an axial surface that sub-parallel the bottom boundary and any irregularities in it. All surface flows of ductile fluids over frictional substrates, such as lavas, salt and polymers, must involve a tank-track fold with a lower limb that inverts the general stratigraphy of the extruded sequence.

Colour layers in most salt extrusions in Iran have major reclined and recumbent flow folds with similar-type profiles (class 2: Ramsay, 1967) in the upper limb of their kinematic tank-track fold. Qom Kuh has about eight major flow folds in a centred S–N profile (Fig. 1C). These folds have axes that sub-parallel the flow front and

are circumferential about the near-summit spreading centre. An axial plane foliation parallels their axial surfaces and defines the particle movement paths in down-flow profiles (Talbot, 1979). Following experimental studies of viscous extrusions, Talbot and Aftabi (2004) attributed the initiation of each of these inclined and recumbent dynamic flow folds to particle movement paths crossing passive marker layers. Flow paths cross markers when the rates at which the fluid extrudes from its vent changes relative to the rate at which it gravity spreads over its surroundings. It is impractical to separate any tectonic signal (the stresses driving extrusion) from the climatic signal (which affects the rate of gravity spreading) on salt fountains like Qom Kuh. However, three salt diapirs on the boundaries of the lithospheric plate on which Qom Kuh occurs have been converted into simple gauges of their driving stresses by being bevelled by sea levels at known times. Thus Mount Sedom was truncated by the Dead Sea at  $\sim 14 \text{ Ka}$  (Weinberger et al., 2006) and the diapirs of Namakdan and Hormoz Island in the Hormoz straits were bevelled by the Persian Gulf at  $\sim 9 \text{ Ka}$  (Bruthans et al., 2006). Despite involving salt sequences of two different ages, all three diapirs are reported to have extruded at much the same steady rates (near  $7 \text{ mm a}^{-1}$ ) for several millennia. The long-term steady extrusion rate for Mount Sedom is particularly remarkable because it extrudes from a fault along which major earthquakes occurred for thousands of years but ceased about 200 years ago (Ambraseys and Jackson, 1998). A steady rate of extrusion from a fault subject to changes in tectonic stresses indicates clearly that gravity is the main force driving these salt extrusions. It follows that if changing tectonic forces can be neglected, then the eight major flow folds on Qom Kuh probably record millennia scale alternations of wet and dry climatic intervals.

Monitoring the movements of markers on different parts of Qom Kuh finds them to move back and forth on time scales from minutes to months or even (locally) years. These elastic strains indicate that the salt expands on heating and contracts on cooling as expected; however the salt also expands on wetting and shrinks on drying. Marker movements are therefore complicated because salt temperatures fall when it rains and rise when the salt dries in the sun. In general, thermal expansion and contraction dominates the swelling and shrinkage of the salt. Large as they are, the elastic strains are eventually exceeded by permanent ductile strains that accumulate when the salt is damp.

## 3. Salt mechanics

Pure rock salt confined by loads  $> \sim 10 \text{ Pa}$  deforms as a crystalline viscous fluid with a viscosity between  $10^{16}$  and  $10^{18} \text{ Pa s}^{-1}$  depending on its purity, grain size, temperature and water content (e.g. Cristescu and Hunsche, 1998). Salt in subsurface diapirs is characterised by a uniformly coarse grain size (1–5 cm) that allows it to flow by dislocation processes at differential diapiric stresses  $> 2 \text{ MPa}$ . Such salt is too strong to flow at the low stresses ( $< 0.4 \text{ MPa}$ ) involved in gravity spreading over the surface (Schledler and Urai, 2007). This section explains how extruded salt deforms to a different, weaker material than diapiric salt (Cristescu and Hunsche, 1998).

Like other subaerial salt extrusions in Iran, the salt extruded at Qom Kuh has gneissose fabrics with bimodal grain sizes. Megacrysts centimetres across surviving from the diapir decrease downslope in size and number as their cores dynamically recrystallise and shed mantles of smaller daughter grains ( $< 1 \text{ mm}$ ) that can form most of the distal salt (Talbot, 1981). Decimetre-thick zones of uniformly fine-grained (0.6 mm) mylonitic salt occur along the lower limbs of major recumbent folds and near (seldom at) the base of most allochthonous salt (although this is not exposed at Qom Kuh). Such mylonite zones appear to detach the overlying

gneissose salt flowing downslope from static salt infilling irregularities along the bottom boundary of the salt (Talbot, 1979, 1981). The micro-fabrics in such mylonite zones indicate that they deform by solution precipitation creep and their sub-grain sizes suggest that they are capable of the rapid strain rates ( $10^{-10} \text{ s}^{-1}$ ) at the low differential stresses ( $<0.4 \text{ MPa}$ ) and surface temperatures of around  $20^\circ \text{ C}$  encountered by extruded salt (Schleder and Urai, 2007). Such rapid flow has been confirmed by field measurements after recent rain (Talbot and Rogers, 1980).

The rheology of natural salt depends on the scale of measurement. Thus, the fit of profile outlines of subaerial salt extrusions in Iran to profiles of viscous fountains and droplets demonstrate that their salt can be treated as a linear viscous fluid on the scale of km (Talbot, 1998). The map form of layering on the surface of namakiers indicate that, on the scale of hundreds of metres and less, the salt deforms as a strain softening fluid with a stress exponent of  $n = 3$  (Talbot and Jarvis, 1984). The stress exponent of a particular salt can increase as the scale of measurement decreases further so that  $n = 5$  in deforming mine pillars, and  $n = 6\text{--}7$  in laboratory specimens (Cristescu and Hunsche, 1998). These empirical findings can be rationalised by assuming that the lithological differences that affect deformation on scales of hundreds of metres and less, and the crystallographic details and impurities that affect laboratory scale measurements, do not affect salt sequences on scales of km.

#### 4. A brittle carapace of dilated salt

Salt is a crystalline ductile fluid when confined at depth but dilates to a brittle elastic solid when de-stressed on exposure. Superposed on the nearly subhorizontal foliation, surface-parallel de-stressing mode-1 opening fractures and micro-cracks weaken surficial salt and render it vulnerable to wetting by precipitation (rain, snowmelt or even a heavy mist). A water content of 0.01 vol%, or even an increase in humidity of the surrounding air to  $>75\%$ , weakens dilated salt so that it can flow 20 times faster than it can when it is dry. (Cristescu and Hunsche, 1998).

Perhaps because Qom Kuh is so small, it is unusual in displaying major subvertical planar joints that can be traced  $>100 \text{ m}$  over its surface and presumably extend as deep into the salt. These master joints are  $\sim 100 \text{ m}$  apart and can be divided into two patterns. Each pattern consists of two sets of subvertical shear fractures that strike approximately  $30^\circ$  each side of the dilation fractures. One set of dilation fractures strikes N–S and the other W–E. The dilational fractures define the  $\sigma_1\sigma_2$  planes of the stress fields operating during the formation of these regional fracture patterns. The great depth to which they penetrate into the salt suggests that Qom Kuh was jointed by regional stresses when the salt was unusually dry (and thus brittle) to unusual depths at unknown time(s) in the past.

The N–S striking set of regional fractures probably records the current N–S shortening of Iran responsible for the anticline through which Qom Kuh emerges (and the Alborz and Zagros mountain to the N and S: Fig. 1A insert). This N–S oriented regional compression would reactivate the two overlapping NW–SE striking faults that bound the Qom Kuh diapir with a dextral sense of shear opening the rhombic vent along which the salt of Qom Kuh rose and is still rising (Fig. 1A, and Fig. 6 in Talbot and Aftabi, 2004; see also Fig. 29 in Hudec and Jackson, 2007).

Like other bodies of salt exposed in Iran, Qom Kuh has a carapace of brittle dilated salt that is recognisable by fractures that sub-parallel the top free surface (Fig. 2). We attributed such broken carapaces to confined salt de-stressing to its free surface because of exposure, unloading and elastic volume changes imposed by changes in the weather, particularly in temperature.

Salt has one of the highest thermal expansivities of any rock. The standard value of the linear thermal expansivity of salt between

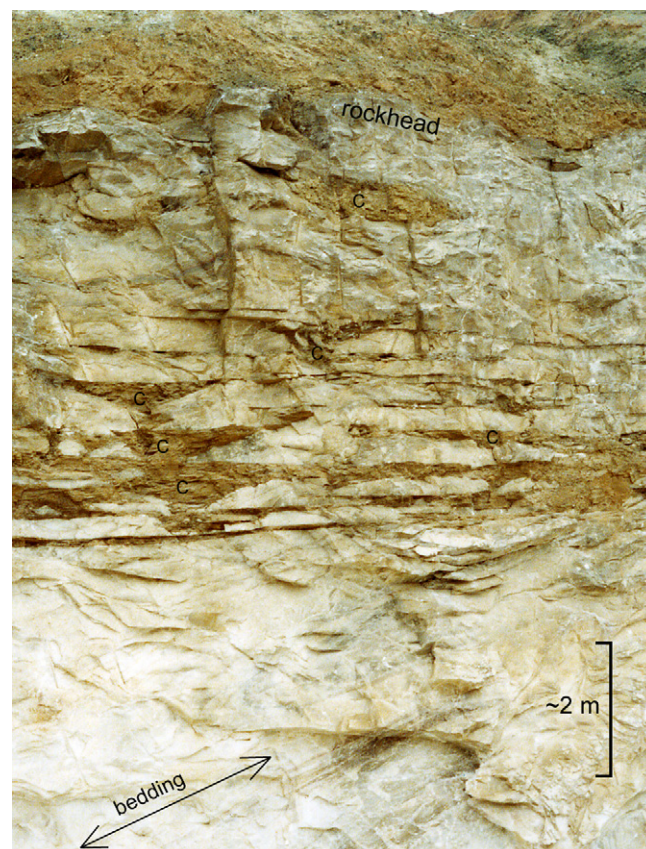


**Fig. 2.** Stress relief fractures newly exposed beneath the irregular top of the salt in Drakhsharnamak quarry ( $35^\circ 14' 20'' \text{ N}$ ,  $52^\circ 09' 00'' \text{ E}$ ) NW Eyvanekey Plateau, 60 km east of Tehran. Most of these fractures, a few decimetres apart, are horizontal and oblique to the salt bedding (indicated); some have been channelled by running water, c, and many are filled by relatively insoluble residual soils washed in from above. The lowest fracture here is unusually long and estimated to be  $\sim 6 \text{ m}$  beneath rockhead (beneath oblique section through gypsite soils). In the upper slopes of a salt fountain like Qom Kuh, the top boundary parallel planar fracture anisotropy may parallel and emphasise a strong gneissose foliation and dies out downward passing into sound salt at depths between 4 and 10 m.

0 and  $107^\circ \text{ C}$  is  $4.2 \times 10^{-5} \text{ K}^{-1}$  (Gevantman, 1981). This has been confirmed to an accuracy of a few % by translating to strains the changes in the distance between two wooden stakes 2 m apart and relating them to the temperature changes on the intervening ground surface on the SE corner of Qom Kuh over a few hours (Aftabi, unpublished MSc thesis, 2000).

The depth ( $D$ ) to which a thermal pulse penetrates the salt is determined by the duration of the pulse ( $\tau$ ) and the thermal conductivity of the salt ( $\kappa$ ), i.e.  $D = (\tau \kappa / \pi)^{-1/2}$  (Turcotte and Schubert, 1982). The equation shows that the skin depth is inversely proportional to the square root of duration of the thermal pulse.

Clean salt is translucent to sunlight but inserting values of thermal diffusivity measured elsewhere of  $3.6 \times 10^{-6} \text{ m}^2 \text{ s}^{-1}$  (Durham et al., 1981) into the expression for the thermal skin depth shows that the diurnal, monthly and annual changes in temperature penetrate about 31.5 cm, 1.7 and 6 m, respectively, into exposed salt (Fig. 3). We infer that thermal shock induced by shrinkage during the cooling phases of increasingly long temperature cycles impart deeper, mainly surface-parallel fractures. Diurnal temperature cycles can result in fractures about 3 dm deep. Shorter-term temperature cycles can result in other fractures closer to the top surface and annual temperature cycles probably fracture exposed salt to depths nearer 6 m (Figs. 2 and 3).

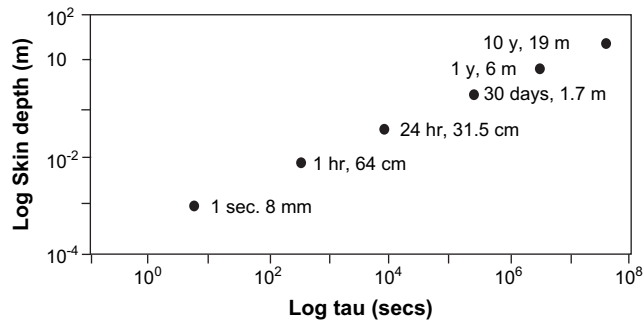


**Fig. 3.** Log thermal skin depth  $(\tau\kappa/\pi)^{1/2}$  (Turcotte and Schubert, 1982), plotted against  $\log \tau$  where  $\tau$  is the regular time interval of the temperature fluctuations on the planar top surface of a semi-infinite half-space of salt with no internal heat source and  $\kappa$  is the thermal diffusivity which for salt is  $3.6 \times 10^{-6} \text{ m}^2 \text{ s}^{-1}$  (Durham et al., 1981). These values suggest that the horizontal joints in Fig. 2 probably formed by thermal shock during mainly annual and diurnal temperature cycles.

Recently quarried vertical salt faces display a surficial zone about 6 m thick of surface-parallel fractures tens of metres long and decimetres apart with or without infillings of gypsiferous soils (Fig. 2, see also other photos in Talbot, 2004). These residual soil infills are the insoluble components left after the salt has been dissolved by water; some may form directly in the fractures but most are washed in from the surface. The deeper fractures in Fig. 2 are unusually long; older exposures in other quarries suggest that such fractures usually increase in spacing, decrease in length with depth, and pass transitionally into sound salt by depths of  $\sim 10$  m.

## 5. Surficial kink and chevron folds on Qom Kuh

We follow the terminology of Ramsay and Huber (1987, p. 442) and refer to folds with narrow angular hinge zones and symmetrical straight limbs of approximately equal length as chevron folds. However, here we will be dealing mainly with a train of folds with planar limbs and angular hinges but will refer to them as kink folds because of their different limb-lengths. The zones defined by the short limbs of kink folds are generally known as kink-bands and their axial surfaces referred to as kink planes.

Relatively minor kink folds in the surficial salt of Qom Kuh are superposed on the colour layers in both limbs of the major similar-style recumbent flow folds and therefore clearly post-date the major folds (see Fig. 4). About 40 individual angular folds were encountered in systematic traverses down the southern slope of Qom Kuh, and nearer 20 (slightly smaller) equivalents down the western slope (Figs. 1 and 5). No attempt was made to follow individual kink folds around the mountain but we will refer to them all as a single train.

Absent on the crest of the dome (and northern and eastern slopes), the highest kink fold seen in each traverse down the flanks of Qom Kuh occurs near the top of the steepest ( $8^\circ$ ) slope as a very gentle asymmetric anticline with an amplitude of a few metres (Fig. 5). The short limb ( $\sim 15$ – $20$  m) dips  $\sim 10^\circ$  downslope and the long limb ( $\sim 50$  m) dips  $\sim 1^\circ$  upslope so the interlimb angle is near  $170^\circ$ . The axial plane joining the angular hinges dips  $\sim 3^\circ$  upslope and parallels a clear grain shape and orientation foliation in the short limb. The wavelength of successive kink folds decreases systematically down the train. Successive hinges begin  $\sim 50$  m apart at the top and decrease to nearer 13 m apart at the bottom. Meanwhile, their amplitudes increase from a few metres to  $\sim 5$  m and their interlimb angles tighten from  $\sim 170^\circ$  to nearer  $90^\circ$ . The short limbs maintain a length near 10 m while the long limbs begin at 50 m and shorten to nearer 10 m as their dips steepen to near  $45^\circ$  as they migrate downslope.

The enveloping surface of the fold train is everywhere sub-parallel to the top surface of the salt. The kink folds are very asymmetric at the top of the train where the enveloping surface is steepest and increase in symmetry downslope to become upright symmetrical chevron folds (with limb-dips of  $\sim 45^\circ$ , and interlimb angles  $\sim 90^\circ$ ) where the enveloping surface becomes subhorizontal in the most distal 200 m or so of salt beyond the base of the slope. An axial planar foliation is present in the short limb of the kink fold at every stage. This axial foliation progressively steepens downslope from very gentle ( $\sim 3^\circ$ ) at the top of the slope to subvertical on the distal salt (Fig. 5). The subvertical axial plane foliation of the distal upright chevron folds fan gently.

The full thickness of the train of surficial kink folds on Qom Kuh is exposed at only a few localities. However, all observed kink folds maintain their sharp hinges as they diminish in amplitude to die out downwards at depths between  $\sim 4$  and 10 m. We recognised no indications that the angular hinges began with rounded forms, or any of the internal geometric complications (accommodation structures) such as bulbous hinges or saddle reefs reported from other kink folds. Nor did we recognise any sign that the train has glided above a basal detachment.

We consider successive examples in this a train of surficial kink folds as maturing from the least mature example high on the slope to the most mature examples (where surficial soils obscure the top of the terminus) as essentially similar incremental strains accumulate downslope. The last eight or so chevron folds in the train have almost identical geometries suggesting that they have ceased evolving (Fig. 5).

## 6. Genetic model for surficial kink folds on Qom Kuh

The small scale of these relatively young angular folds suggests that they affect only a surficial zone of salt 4–10 m thick (Fig. 5). Their increase in symmetry downslope while maintaining circumferential axes might be attributed to a thin outer layer of competent salt buckling over a weaker interior (like the stiff skin of molten lava: Rowland and Walker, 1987). The provisional explanation by Talbot and Aftabi (2004) was that the surficial zone of Qom Kuh was first dilated and broken by surface-parallel fractures because of thermal shock when it was dry. Then, after this surficial broken layer was dampened and weakened by precipitation, it folded as it moved downslope up to 20 times faster than the underlying, still-confined salt (Talbot and Aftabi, 2004). However, although their analogue modelling study successfully simulated the curtain folds, tank-track fold and major flow folds, they were unable to simulate the trains of minor kink folds superimposed on the surficial salt of Qom Kuh. Moreover, that work missed a key aspect of the surficial folds on Qom Kuh, their angularity. This implies shortening of a planar mechanical anisotropy, a characteristic we emphasise here by referring to them as kink folds.

Like angular folds in other rocks elsewhere, the kink folds at Qom Kuh developed in rock with a well developed planar anisotropy deformed at low (diagenetic to greenschist) metamorphic facies. However, the kink folds at Qom Kuh appear to be unique in that they develop in a clear train that appears to record every stage from their initiation through their progressive maturation to a sequence of upright chevron folds.

This train has important lessons regarding the kinematics and dynamics of angular folds in general. For instance, the angular nature of the least mature example in the train challenges the assumption reached by Bastida et al. (2007) that chevron folds initiate with rounded geometries and only become angular in the later stages of deformation. After their graphic modelling, these authors concluded that chevron folds require a remarkably complicated deformation history with phases of tangential

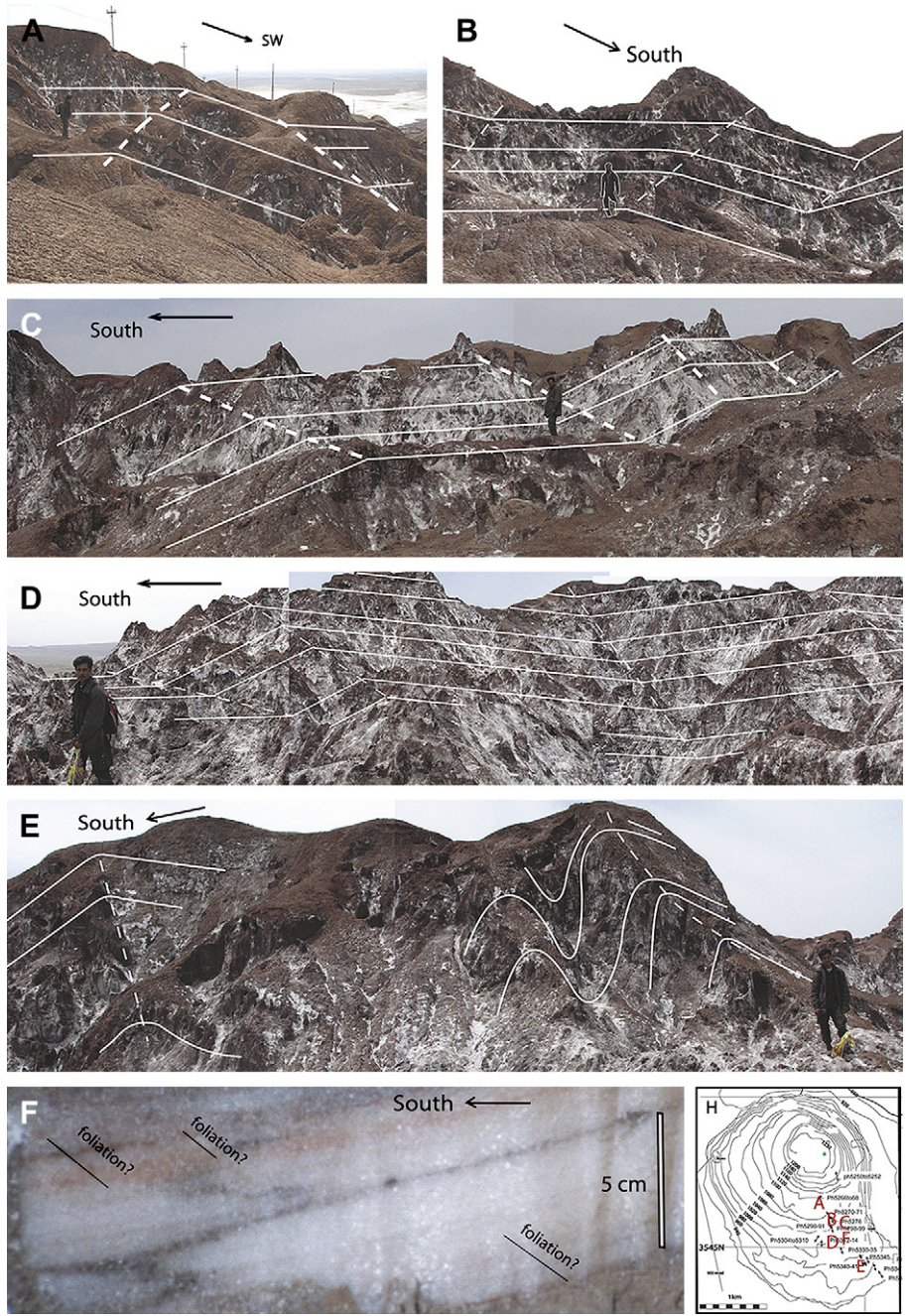


**Fig. 4.** Field photographs of profiles of kink folds and chevron folds on the southern slopes of Qom Kuh with interpreted bedding and axial surfaces complicated by relief. Photos A–E are in approximate order of increasing maturity downslope. The close up F is near D. All photos are located on map G bottom right.

longitudinal strains (with and without volume change) and flexural flow (with or without a preceding phase of longitudinal shortening and a following phase of homogeneous strains). Bastida et al. (2007) considered that the homogeneous strains at the beginning and end of folding may not be necessary whereas the other three stages “appear to be essential”. However, they assumed that their folds began rounded and remained rounded until their interlimb angle became  $<120^\circ$ . These authors accepted that “once the chevron shape has developed it could then amplify by homogeneous strain alone”. They also accepted that isochoric layer parallel longitudinal strain produces perfect chevrons with a cleavage fan but appear to have ruled out this simple model because of the high strains involved ( $>70\%$  shortening for interlimb angles  $<90^\circ$ ).

Work on the buckling of anisotropic materials (see e.g. Biot, 1961, 1964, 1965; Cobbold et al., 1971; Cosgrove, 1976) demonstrates that two types of buckles can develop when such a material is compressed along the fabric defining its planar mechanical anisotropy. These are folds with axial planes at  $90^\circ$  to the compression direction and box folds (conjugate kink-bands) with axial planes oblique to the maximum compression direction (Fig. 6). Subsequent work by Cobbold (1976) and Summers (1979) showed that, as these structures amplify, the fold limbs become progressively straighter and, as a consequence, the folds become more angular. The result is that the folds take on chevron geometry and the box folds rapidly become angular so that they display steeply dipping straight limbs. In addition, if the loading conditions

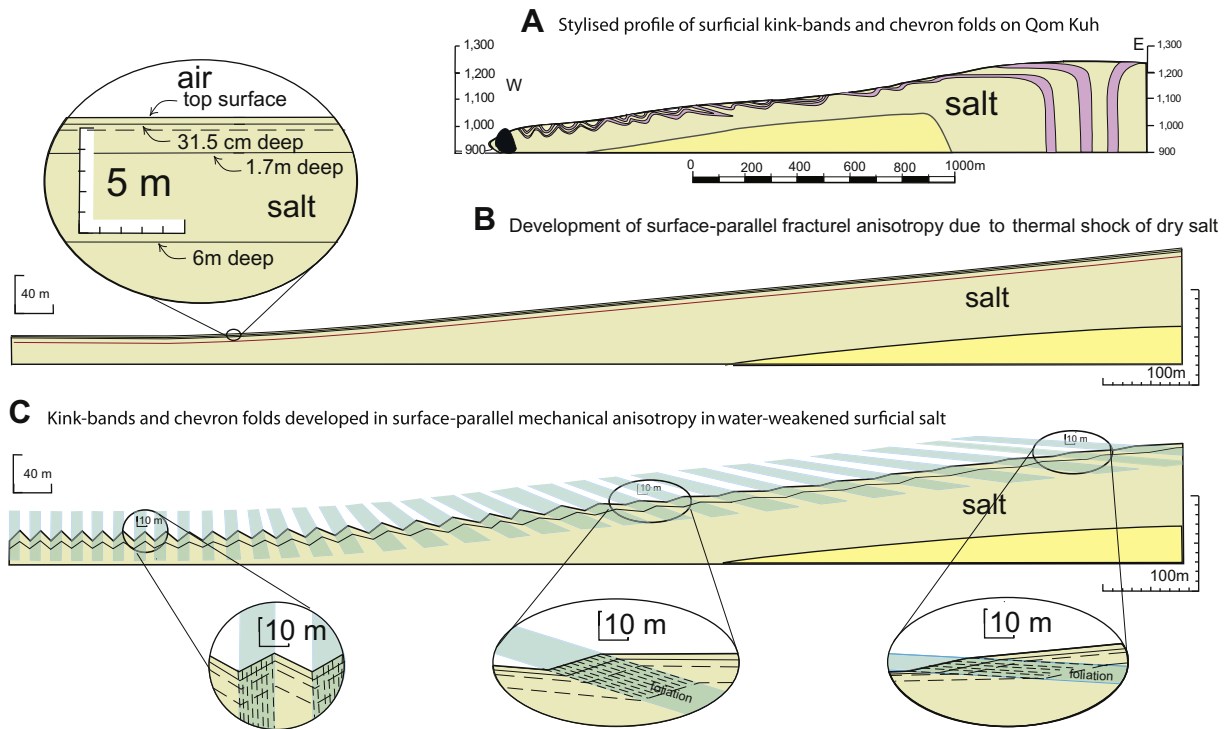


**Fig. 5.** Stylised W–E profiles of Qom Kuh indicating how a train of kink and chevron folds affects an anisotropic carapace of salt. (a) Stylised profile of surficial kink-bands and chevron folds superposed on major recumbent flow folds (not shown). (b) Surface-parallel fracture induced anisotropy developed in dry surficial salt by thermal shock and (c) kink-bands and chevron folds with their foliation developed in the surface-parallel anisotropy in surficial salt when it is weakened by rain.

are not symmetrical (i.e. if the maximum principal compressive stress is oblique rather than parallel to the fabric), then one set of the conjugate kink-bands that define the box fold in Fig. 6B is suppressed and the deformation will be dominated by a single set.

The rounded geometries of the curtain folds, tank-track fold and major flow folds in the main body of Qom Kuh contrast with the angularity of its surficial kink folds. We interpret this marked contrast to be a direct reflection of the mechanical properties of the salt at the time of folding. During diapiric intrusion and large-scale post-extrusion gravity spreading, the salt deforms as an approximately homogeneous, isotropic, ductile material and the colour banding in the salt acts primarily as a passive marker. (Here we neglect the blocks of lava that emerge already dispersed on the summit dome and which are carried downslope to ground near the southern terminus (Figs. 1B,C). The fact that we recognised no complications associated with these 10–100 m scale blocks suggests that most of them had already lodged near the terminus before the kink folds began to form). There was no major contrast in material properties between the various coloured layers and the resulting folds simply record the ductile flow of the salt during intrusion and extrusion. In contrast, the angular geometry of the kink folds indicates clearly that the surficial salt possessed a significant planar mechanical anisotropy during their formation. We attribute this anisotropy to the surface-parallel fractures that develop in the surficial salt of Qom Kuh when it is dry (Fig. 2).

A single set of strongly asymmetric kink folds develops in the anisotropic carapace on Qom Kuh where it reaches dips of  $8^\circ$  on the flanks of the summit dome. It is argued that gravity is the main driving force for this deformation and that the folds form in response to lateral compression and shear. As the folds migrate down the flank of the salt body, the dip of their axial surfaces increases and becomes subvertical in the subhorizontal surficial distal salt that is characterised by upright chevron folds. The model is similar to that for gravity gliding systems in other rocks but

differs in that the extensional faults that characterise the upper slopes of most gravity glide systems are absent. We suggest that the reason for this is that the boundary conditions at Qom Kuh and the rheology of the salt are different. We argue that there is no basal detachment beneath the surface carapace and that the brittle extension deformation that characterises the upslope zones of classical gravity detachment complexes is replaced by ductile extension seen in the form of a strong, subhorizontal foliation in the salt exposed on the summit dome. The planar anisotropy in the surficial salt dies out by a depth near 10 m and there is no detachment separating the kinked zone from the underlying salt. We assume the longitudinal shortening and shear taken up by the kink folds in the surficial salt continues downward but become ductile in the unknicked salt layers beneath.

The formation of just one set of kink folds rather than a conjugate pair (Fig. 6B) reflects the fact that the principal compression is not acting exactly along the anisotropy. In a more conventional gravity glide system very little shear stress can develop above the usual basal detachment. Consequently the principal stresses act either parallel to or normal to the layering and so the structures that form tend to be symmetric. However, in the system under consideration, the anisotropic carapace is not separated from the underlying salt by a detachment but merges with the main body of the salt. Thus, the gravity-generated downslope compression and shear is not constrained to acting exactly along the layering with the result that just one set of kink-bands forms.

## 7. Forward modelling of kink folds on Qom Kuh

We assume that layered salt with very low competence contrasts between the layers develops a planar mechanical anisotropy parallel to the salt/air interface as it extrudes and dilates on exposure. This change is restricted to the surface of the exposed salt and penetrates only a few metres into the salt body. The mechanically

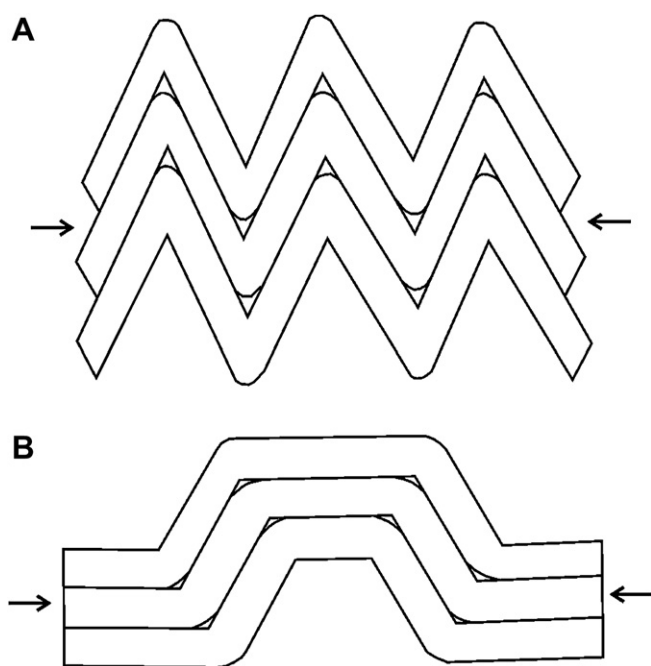


**Fig. 6.** Two modes of buckling of a mechanically anisotropic material compressed parallel to the layering or fabric making up the anisotropy. (A) Upright chevron folds with axial planes normal to the maximum compression. (B) A box fold made up of a conjugate pair of kink-bands with axial planes oblique to the maximum compression. After Price and Cosgrove (1990, Fig. 13.7).

anisotropic carapace to the salt body buckled as the body of salt spread under gravity. We assume that the low-amplitude, sharp-hinged kink folds that characterise the upper slopes of the dome (Figs. 1 and 5) were the first to form and, using the graphics program in “Adobe Illustrator” ©, consider in axial profiles the effect of applying a horizontal homogeneous shortening combined with a horizontal shear on the geometrical evolution of these early folds. Fig. 7 illustrates the results separated into three isochoric phases that in nature would act together, i.e. horizontal pure shear shortening, with horizontal simple shear, and gravity.

Whilst acknowledging that folding usually involves an element of both active and passive amplification (see e.g. Fig. 10.17 in Price and Cosgrove, 1990), the following simulations ignore any active buckling of the carapace that follows the formation of the initial structure at the top of the slope.

The diagrams at the right hand ends of both Figs. 7A,B represents the highest kink fold recognised in the train with its short limb dipping  $10^\circ$  downslope, the layering within its long limb dipping  $1^\circ$  upslope and its axial surface (and foliation) dipping  $3^\circ$  upslope. Successive diagrams to the left in Fig. 7A illustrate four progressive strain increments each of which involves 20% horizontal shortening by pure shear. This can be seen by following the distortions of the circle and square superposed on the initial kink fold. Fig. 7A accounts for some of the aspects of the train of kink folds on Qom Kuh but the left hand diagram is not the upright chevron fold seen in the most distal examples on Qom Kuh (Fig. 5). Fig. 7A needs another component of strain to explain the downslope surficial structures on Qom Kuh.

Fig. 7B adds four equal increments of  $10^\circ$  of horizontal homogeneous simple shear to each increment illustrated in Fig. 7A. This represents the affect of the shear stress imposed across the anisotropic carapace by the outward flow of the underlying salt. Although Fig. 7B neglects the likelihood that increasing volumes of the salt of Qom Kuh are lost downslope to dissolution, it successfully captures the essential geometry of the train of kink and chevron folds.

Talbot and Aftabi (2004) assumed that the carapace of Qom Kuh moved faster than the underlying confined salt whereas the simple shear invoked in Fig. 7B implies that the surface does not move as fast. However, the shear associated with a slower top surface assumed in Fig. 7B is consistent with the classical internal flow profile of a viscous extrusion spreading under gravity illustrated in Fig. 7C. This shows the shear couples generated by gravity spreading over a horizontal base acting across a stronger, thin, brittle carapace and the basal contact. Experiments by Gilbert and Merle (1987), confirmed that finite stretch trajectories on the top surface of radially spreading extrusions of silicone putty are concentric and parallel to the flow front downstream of a zone of no finite stretch (at the upper limit of the train of kink folds). Finite stretch trajectories are radial and parallel to the flow direction upstream (upslope of the point where the kink folds initiate). The incremental stretch on the top surface-parallel the flow front everywhere.

Fig. 7D is an expansion of Fig. 7B and applies 20 equal increments, each of 4% horizontal shortening by pure shear with  $2^\circ$  horizontal simple shear, to the geometry of the kink fold beside it upslope. The resulting kink folds are arranged so that the top surface is continuous. Only one distal chevron fold is shown because we follow de Sitter (1958) and assume that the interlimb angles of the most distal chevron folds on Qom Kuh indicate that these folds have ceased to evolve and have merely accumulated there.

The fold train modelled in Fig. 7D is horizontal. Assuming that gravity ensures that the fold train follows the topographic slope, the train modelled in this figure has been deformed in Fig. 7E to an approximate fit to the western slope of Qom Kuh by subjecting the upper and middle thirds to  $6^\circ$  and  $3^\circ$  left-handed vertical simple shear respectively. In addition, the gaps in the bottom boundary of the fold train in Fig. 7E have been closed in Fig. 7F to form a continuous bottom boundary smoother than the top boundary to portray a fold train that dies out downward. This figure demonstrates that the train of kink folds in the surficial salt of Qom Kuh can be modelled realistically by adding progressive equal increments of isochoric horizontal shortening by pure shear and horizontal simple shear with gravity fitting the kink folds to the slope. The three components of strain shown separately here would have acted contemporaneously in nature.

Bastida et al. (2007) balked at invoking layer parallel longitudinal strain to account for kink folds because it would involve  $>70\%$  shortening to reach interlimb angles  $<90^\circ$ . Our strains are not quite layer parallel and the 80% lateral shortening and 40% simple shear invoked for the generation of the distal chevron folds may seem very high. However, to add some perspective, the gravity driven strains we invoke to account for the surficial train of kink folds pale by comparison with those involved with the emplacement of the salt that kinked. Gravity drove the most distal salt to its present position several km along its source layer (probably  $<1$  km thick), 3 km up the diapiric vent ( $>1$  km across), and about 2 km downslope over the surface in an allochthonous salt sheet less than 200 m thick (Fig. 1). Thus, the kink folding is a relatively minor final adjustment to intense strain of the complete salt body.

## 8. Discussion

### 8.1. Rate of shortening

We do not know how long a chevron fold takes to develop on Qom Kuh – nor whether new ones are still forming. However, Qom Kuh is readily accessible and it should be possible for others to find out.



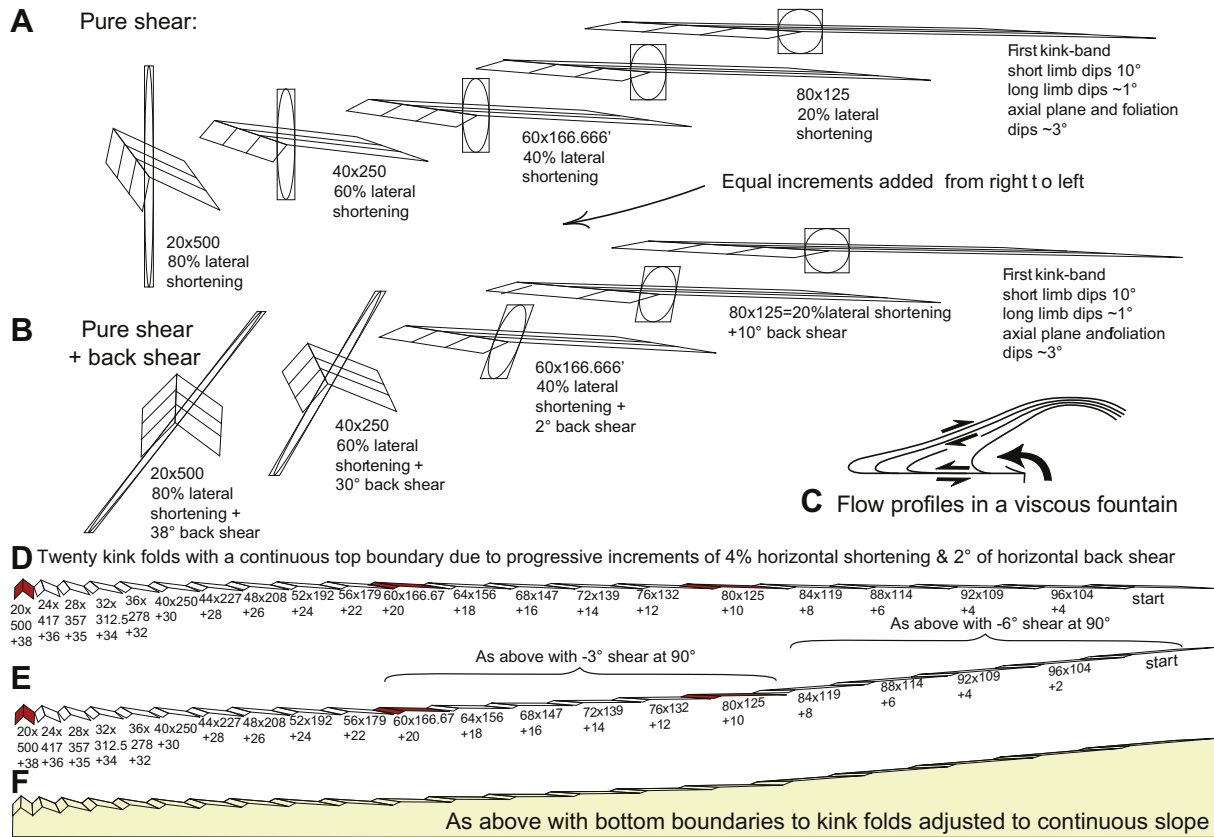


**Fig. 7.** A simple forward kinematic model of the strains involved in the formation of the angular structures in the surficial salt of Qom Kuh, divided into four components. (A) Isochoric pure shear is added in four equal increments of 20% horizontal shortening to a circle and square added to a diagrammatic representation of the least mature kink fold at the top of the train to the right (cf. Fig. 6). (B) Four equal increments of isochoric horizontal right-handed simple shear by 10° are added to each of the increments in A to simulate most aspects of the angular structures on Qom Kuh. (C) Part of the flow profile of a viscous fountain gravity spreading over a horizontal non-slip surface to illustrate back-shear across the top boundary between the flowing salt and the overlying, more brittle carapace. (D) Twenty kink folds to the left of the least mature kink fold (right hand diagram in A & B) incorporating progressive equal increments of 4% horizontal shortening by pure shear together with 2% simple back-shear. The darkened increments are those shown in B. The figures beneath each fold are the horizontal and vertical scale values applied to the starting fold to generate each increment. (E) As in D but taking account of the slope by adding 6° left-handed vertical simple shear to the top five increments and 3° left-handed vertical simple shear to the next six increments. (F) As in E but joining the bottom boundary of the folds to a continuous contact with the underlying ductile confined salt.

The top two kink folds are about 50 m apart and, at the long-term rate for the vertical extrusion of salt out of the diapiric vent of  $8 \text{ cm a}^{-1}$  estimated by Talbot and Aftabi (2004), it would take  $5000/8 = 625$  years for the top fold to replace the second. Down-slope movements of markers on the salt of Qom Kuh have been measured at metres in some months so it is not impossible that a new kink fold could form in a few wet years. The dramatic 80% lateral shortening in the bottom eight chevron folds implied by our analysis (Fig. 7) would involve a strain rate of  $5.3 \cdot 10^{-11} \text{ s}^{-1}$  if the whole train formed in the 42,000 years that Talbot and Aftabi (2004) estimated it took to extrude the current salt.

The percentage lateral shortening between successive chevron folds modelled in Figs. 7E,F is 4%. For one chevron fold to move 50 m downslope to replace another in a year would imply an unlikely fast strain rate near  $8 \cdot 10^{-8} \text{ s}^{-1}$ . We therefore prefer the idea that one chevron fold replaced the next in  $\sim 625$  years. This implies a strain rate near  $5 \cdot 10^{-9} \text{ s}^{-1}$ , not far from the  $10^{-10} \text{ s}^{-1}$  allowed by the sub-grain sizes in a salt mylonite from the same region (Schleder and Urai, 2007).

## 8.2. Kinking by traction, not direct gravity induced stresses

The model developed in Fig. 7 is the simplest of many empirical attempts to generate the basic pattern of the train of kink and chevron folds illustrated in Fig. 5. Notice that the increments of

isochoric shortening and shear are horizontal, parallel to the bottom boundary of the allochthonous salt at Qom Kuh and oblique to the top boundary. The obliquity of the stress associated with this deformation to the planar anisotropy accounts for the development of a single train of kink folds. Attempts to model the reverse situation (isochoric shortening and shear parallel to the top slope of the salt and oblique to the bottom boundary) were markedly unsuccessful. The geometry of the strains in Fig. 7 imply strongly that the force driving the kinking was not the force of gravity acting directly on the inclined anisotropic layer. Instead, the horizontal compression and shear stresses responsible for the kink folds are due to traction with the underlying salt mass that is gravity spreading over a horizontal no-slip bottom boundary. This interpretation is compatible with the idea that the strength of the anisotropic carapace hinders gravity spreading of the salt mass when it is dry but allows gravity spreading when the carapace weakens and kinks on wetting.

## 8.3. Superposition of new on old foliations

Grain shape and orientation fabrics in diapiric salt flowing steadily with a unimodal grain size deform smoothly from one strain regime to another (e.g. from planar to linear fabrics: Schmeling et al., 1988). Consequently, only a single grain shape fabric is usual at any one location in diapiric salt. This has been

attributed elsewhere (Talbot and Jackson, 1987) to every grain in a steadily flowing monomineralic rock mass being competent compared to its surroundings networked by grain boundaries. This means that every grain can rotate through a range of orientations and ellipticities by supershear and maintain a constant foliation defined by the orientation at which every constituent grain reaches its maximum ellipticity. Supershear of its constituent grains allows gneissose salt flowing steadily along a flow line to maintain a steady state foliation and grain size (Talbot and Jackson, 1987).

By contrast, the bimodal grain sizes of extruded salt can develop multiple grain shape fabrics in some situations. Thus a coarse subvertical crenulation cleavage defined by decimetre-scale chevron folds is clearly superposed on the diapiric foliation where its sheet dip is subhorizontal (Talbot, 2004, Fig. 5) between the steep foliations in the core and margin of dome 28 among the Semnan diapirs in the Great Kavir (Jackson et al., 1990). Similarly, field sketches in Talbot (1979), (Fig. 5) illustrate a stack of minor folds that become increasingly asymmetric downward until their short limbs become mylonitic shear zones.

One might therefore expect multiple foliations on Qom Kuh: (1) where the steep (3D linear?) grain shape fabric that emerges from the diapiric vent is replaced by the subhorizontal planar fabric that defines the foliation in the summit dome of Qom Kuh; and (2) where new foliations develop axial planar to folds down the flanks of the Qom Kuh.

We did not study the superposition of new on old foliations on Qom Kuh. However, we expect them to simulate the process reported in two dimensions from deep in the Hormoz salt of Kuh-e-namak (Dashti) at 28°17'N, 51°43'E by Talbot (1979), pp. 10–14 and Figs. 4c and 6. The new foliation there fanned slightly about the axial surface of a minor asymmetric fold developed on the limb of a major flow fold. The old foliation was axial planar to the major fold and sub-parallel to the bedding in its limb.

The long axes of megacrysts and the contours of size and megacryst ellipticity defined the old foliation where it was undisturbed by the minor fold. In the new fold, the long axes of megacrysts and these contours paralleled the new foliation that dipped 40–50° more steeply than the old foliation. In transitional zones <10 cm wide, where the bedding was rotated between 1 and 20° into the new fold, the megacrysts had low ellipticities with “long” axes at high angles to both the old and new foliations.

Instead of the old foliation smoothly turning into the new foliation by megacrysts increasing in aspect ratio as they rotated, the megacrysts reached long/short axial ratios between 3:1 and 5:1 before separating to form a row of three or four smaller megacrysts with long axes nearly perpendicular to the long axis of the initial megacryst. The maximum aspect ratio reached was >3:1 where rotation was significant and 4:1 where it was not. This breakage of old elliptical megacrysts of cubic halite to smaller megacrysts with low ellipticity means that deforming bimodal salt is continually seeded with “undeformed” sub-circular megacrysts. In effect, such breakage anneals the old foliation and allows a new foliation with another orientation to appear across transition zones <10 cm wide. This process implies that salt with bimodal grain size has grain shape fabrics with very short strain memories (Talbot, 1979). Consequently, we made no attempt to measure finite strains anywhere on Qom Kuh.

Significant penetrative flow of extruded salt is episodic and confined to the few days or weeks a year when the salt is damp. The flow lines of each new episode of flow may cross passive bedding inherited from the previous episode and generate new flow folds. Where the new flow lines crosses bedding, the new folds and their axial foliation parallel to the new flow lines emerge out of regimes characterised by the old foliation. We therefore expect foliations axial planar to the flow folds and kink folds down the flanks of Qom

Kuh to emerge abruptly out of the bedding parallel foliations in the deeper salt.

## 9. Summary

Qom Kuh maintains a steady profile because gravity spreads salt over a rigid base at about the same rate as it extrudes and dissolves as a visco-elastic crystalline material. The steady shape is that of a smooth rounded viscous fountain (Figs. 1, 5 and 7). Markers on the salt surface accumulate permanent downslope displacements of decimetres over years when the salt is damp despite undergoing elastic strains equally large over a day or less when the salt is dry. Gravity spreading in the viscous fountain imposes a top boundary parallel gneissose foliation generated by extension at the flow separation point in the summit (Figs. 1B,C).

Like other bodies of salt exposed in Iran, the outer 4–10 m of salt on Qom Kuh de-stresses to the top free surface when it is dry and exfoliates by unloading. Such de-stressing dilates a brittle carapace characterised by surface-parallel planar fractures ( $\pm$ soil infills). Qom Kuh is the only salt extrusion in Iran where the outermost 4–10 m of surficial salt (on the southern and western flanks) is known to develop kink folds. However, Qom Kuh is also the only salt fountain examined in detail on the central plateau of Iran. The formation of such folds on the slopes of the salt where the lateral component of stress must be very low, suggests that the salt must have been relatively weak in order to kink. It is argued that these kink folds developed in the dilated, mechanically anisotropic carapace, when it was weakening drastically on wetting.

The model proposed is one in which a planar, mechanical anisotropy formed in dry surficial salt by fracturing parallel to the surface of the salt as a result of thermal shock on time cycles of a year and less. These surface-parallel fractures die out downwards so the dilated carapace is welded to the underlying confined salt. When it is dry, the carapace acts as a strong elastic strut that inhibits the ductile downslope flow of the salt beneath it. With precipitation, the strut weakens considerably and no longer has the strength to prevent flow of the underlying confined salt. The resulting stresses (<0.4 MPa) cause the strut to fold and its anisotropic properties determine that the type of folding it develops is kink folding. This model predicts that the downslope flow of the salt will be inhibited during dry intervals and will occur dominantly during wet intervals. Although the surface-parallel foliation over the summit dome of Qom Kuh might have formed by rotation from a steep grain shape fabric in the diapir, we attribute it to lateral extension: in either case, it replaces the extensional faults usual in the upper levels of detached gravity glide systems in other rocks.

Rather than gravity spreading by the bulk creep process that generates a penetrative foliation in the underlying salt, the anisotropic carapace of Qom Kuh develops kink folds because of the lateral shear and compression transferred by traction from the underlying ductile spreading salt. During wet weather, existing asymmetric folds move downslope and amplify to the symmetrical upright chevron folds that accumulate in the horizontal distal salt. Meanwhile new asymmetric kink folds are assumed to develop at the head of the train on the upper slopes. Further work may constrain how long it takes individual folds to develop and mature but there is no reason to doubt that new folds are still forming.

## 10. Conclusions

This work has suggested that the planar mechanical anisotropy generated in the superficial crust of salt extruded at Qom Kuh plays an important role in the rate at which gravity spreading occurs. When it is dehydrated, the carapace is relatively strong and acts as a stiff corset impeding downslope flow of the underlying confined

salt. When it is weakened by water, it can no longer resist salt movement and deforms together with the underlying salt. The relatively isotropic body of confined salt with which it merges at depth deforms by penetrative bulk flow whereas the significantly anisotropic carapace deforms by developing kink folds.

### Acknowledgements

We thank Martin Jackson for his constructive and thoughtful review that improved our presentation. We also thank Dr Korehei, the General Director of the Geological Survey of Iran and his colleagues, for their enthusiastic encouragement and considerable logistic support for our month long visit to Iran early in 2004 during which we visited Qom Kuh in the company of several Iranian and foreign geologists (including Martin Jackson, Jean Letouzey and Hemin Koyi). The Swedish Natural Science Foundation funded CT's travels between Sweden and Iran. P.A. thanks the Swedish Institute for funding his 9-month research visit to Uppsala.

### References

- Aftabi, P., 2000. Salt tectonics of the Qom Kuh, Central Iran. MSc thesis. Institute of Earth Sciences, Geological Survey of Iran, PO box 131851-1494, Tehran, Iran, 421 pp (in English and Farsi).
- Ambraseys, N.N., Jackson, J.A., 1998. Faulting associated with historical and recent earthquakes in the eastern Mediterranean region. *Geophysical Journal International* 133, 390–406.
- Bahroudi, A., Talbot, C.J., 2003. The configuration of the basement beneath the Zagros basin. *Journal of Petroleum Geology* 26, 257–282.
- Bastida, F., Aller, J., Toimil, N.C., Lisle, R.J., Bobillo-Ares, N.C., 2007. Some considerations on the kinematics of chevron folds. *Journal of Structural Geology* 29, 1185–1200.
- Beaumont, C., Jamieson, R.A., Nguyen, M.H., Lee, B., 2001. Himalayan tectonics explained by extrusion of a low-viscosity crustal channel coupled to focused surface denudation. *Nature* 414, 738–742.
- Biot, M.B., 1961. Theory of folding of stratified visco-elastic media and its implications in tectonics and orogenesis. *Geological Society of America Bulletin* 72, 1595–1620.
- Biot, M.B., 1965. *Mechanics of the Incremental Deformations*. Wiley, New York, 504 pp.
- Bruthans, J., Bruthans, J., Filippi, M., Gersl, M., Zare, M., Melkov, A.J., Pazdur, A., Bosak, P., 2006. Holocene terraces on two salt diapirs in the Persian Gulf (Iran): age, depositional history and uplift rates. *Journal of Quaternary Geology* 21, 843–857.
- Cobbold, P.R., 1976. Mechanical effects of anisotropy during large finite deformations. *Bulletin de la Societe Geologique de France* 7, 1497–1510.
- Cobbold, P.R., Cosgrove, J.W., Summers, J.M., 1971. Development of internal structures in deformed anisotropic rocks. *Tectonophysics* 12, 23–53.
- Cosgrove, J.W., 1976. The formation of crenulation cleavage. *Journal of Geological Society of London* 132, 155–178.
- Cristescu, N., Hunsche, U., 1998. *Time Effects in Rock Mechanics – Series: Materials, Modelling and Computation*. John Wiley and Sons, Chichester.
- de Sitter, L.U., 1958. Boudins and parasitic folds in relation to cleavage and folding. *Geologie en Mijnbouw* 20, 277–286.
- Durham, W.B., Abey, A.E., Trimmer, D.A., 1981. *Thermal Conductivity and Diffusivity and Expansion of Avery Island Salt at Pressure and Temperature*. Technical Report University of California, Lawrence Berkley Laboratory, Livermore, CA, USA.
- Gevantman, L.H. (Ed.), 1981. *Physical Properties Data for Rock Salt*. US Dept. Commerce NBS Monograph 167, p. 214.
- Gilbert, E., Merle, O., 1987. Extrusion and radial spreading beyond a closing channel. *Journal of Structural Geology* 9, 481–490.
- Hudec, M.R., Jackson, M.P.A., 2007. Tera Infirma: understanding salt tectonics. *Earth Science Reviews* 882, 1–28.
- Huppert, H.E., 1982. The propagation of two-dimensional and axisymmetric viscous gravity currents over a rigid horizontal surface. *Journal of Fluid Mechanics* 121, 43–58.
- Jackson, M.P.A., Cornelius, R.R., Craig, C.R., Gansser, A., Stöcklin, J., Talbot, C.J., 1990. Salt diapirs of the Great Kavir, central Iran. *Geological Society of America Memoir* 177.
- Lister, J.R., Kerr, R.C., 1989. The propagation of two-dimensional and axisymmetric viscous gravity currents at a fluid interface. *Journal of Fluid Mechanics* 203, 215–249.
- Player, R.A., 1969. Salt plug study. Iranian Oil Operating Companies, Geological and Exploration Division, Report No 1146 (unpublished).
- Price, N.J., Cosgrove, J.W., 1990. *Analysis of Geological Structures*. Cambridge University Press, Cambridge, 502 pp.
- Ramberg, H., 1981. *Gravity, Deformation and the Earth's Crust*, second ed. Academic Press, London, 452 p.
- Ramsay, J.G., 1967. *Folding and Fracturing of Rocks*. McGraw Hill, New York.
- Ramsay, J.G., Huber, M.L., 1987. *The Techniques of Modern Structural Geology*. In: *Folds and Fractures*, Vol 2. Academic Press, London, 462 pp.
- Rowland, S.K., Walker, G.P.L., 1987. Toothpaste lava: characteristics and origin of a lava structural type transitional between pahoehoe and aa. *Bulletin of Volcanology* 49, 631–641.
- Schleder, Z., Urai, J.L., 2007. Deformation and recrystallization mechanisms in mylonitic shear zones in naturally deformed extrusive Eocene–Oligocene rocksalt from Eyvanekey plateau and Garmsar hills (central Iran). *Journal of Structural Geology* 29, 241–255.
- Schmeling, H., Cruden, A.R., Marquart, G., 1988. Finite deformation in and around a fluid sphere moving through a viscous medium: implications for diapiric ascent. *Tectonophysics* 149, 17–34.
- Sepehr, M., Cosgrove, J.W., 2005. The role of the Kazerun Fault Zone in the formation and deformation of the Zagros Fold-Thrust Belt, Iran. *Tectonics* 24, TC5005. doi:10.1029/2004TC001725.
- Summers, J.M., 1979. An experimental and theoretical investigation of multilayer fold development. Unpublished PhD thesis, University of London.
- Talbot, C.J., 1979. Fold trains in a glacier of salt in southern Iran. *Journal of Structural Geology* 1, 5–18.
- Talbot, C.J., 1981. Sliding and other deformation mechanisms in a salt glacier. *Iran. Geological Society of London Special Publication* 9, 173–183.
- Talbot, C.J., 1998. Extrusions of Hormoz salt in Iran. In: Blundell, D.J., Scott, A.C.A. (Eds.), *Lyell: The Past is the Key to the Present*. Geological Society of London. Special Publications, vol. 143, pp. 315–334.
- Talbot, C.J., 2004. Extensional evolution of the Gulf of Mexico basin and deposition of tertiary evaporite: discussion. *Journal of Petroleum Geology* 27, 95–104.
- Talbot, C.J., Aftabi, P., 2004. Geology and models of salt extrusion at Qom Kuh, central Iran. *Journal Geological Society London* 161, 321–334.
- Talbot, C.J., Alavi, M., 1996. The past of a future syntaxis across the Zagros. In: Alsop, G.L., Blundell, D.J., Davison, I. (Eds.), *Salt Tectonics*. Geological Society of London, Special Publication, vol. 100, pp. 89–109.
- Talbot, C.J., Jackson, M.P.A., 1987. Internal kinematics of salt diapirs. *American Association of Petroleum Geologists Bulletin* 71, 1068–1098.
- Talbot, C.J., Jarvis, R.J., 1984. Age, budget and dynamics of an active salt extrusion in Iran. *Journal of Structural Geology* 6, 521–533.
- Talbot, C.J., Rogers, E., 1980. Seasonal movements in an Iranian salt glacier. *Science, Washington* 208, 395–397.
- Talbot, C.J., Medvedev, S., Alavi, M., Shahrivar, H., Heidari, E., 2000. Salt extrusion rates at Kuh-e-Jahani, Iran: June 1994 to November 1997. In: Vendeville, B., Mart, Y., Vigneresse, J.-L. (Eds.), *Salt, Shale and Igneous Diapirs in and Around Europe*. Geological Society of London Special Publication, vol. 174, pp. 93–110.
- Turcotte, D.L., Schubert, G., 1982. *Geodynamics: Applications of Continuum Physics to Geological Problems*. Wiley, New York, p. 157.
- Weinberger, R., Begin, Z.B., Waldman, N., Gardosh, M., Baer, G., Frumkin, A., Wdowinski, S., 2006. Quaternary rise of the Sedom diapir, Dead Sea basin. In: Enzel, Y., Agnon, A., Stein, M. (Eds.), *New Frontiers in Dead Sea Paleoenvironmental Research*. Geological Society of America Special Publication, vol. 401, pp. 33–51.